



## Nonlinear energy in a wave turbulence system

Naoto Yokoyama<sup>a\*</sup> and Masanori Takaoka<sup>b</sup>

<sup>a</sup> Department of Aeronautics and Astronautics, Kyoto University, Kyoto 615-8540, Japan

<sup>b</sup> Department of Mechanical Engineering, Doshisha University, Kyotanabe 610-0394, Japan

Received 8 December 2014, accepted 20 May 2015, available online 28 August 2015

**Abstract.** Single-wavenumber representations of nonlinear energies are required to investigate energy budget due to nonlinear interactions among Fourier modes in wave turbulence. While we have reported in a previous paper that the single-wavenumber representations successfully works for the Föppl–von Kármán equation, we will show here that for the Majda–McLaughlin–Tabak model the single-wavenumber representations of nonlinear energies is not necessarily unique. Introducing auxiliary variables composed differently from complex amplitudes, two natural representations of the nonlinear energy are obtained. It is numerically observed that the two kinds of the nonlinear-energy spectra, based on these two representations, are qualitatively similar, but the energy budgets are clearly different. To select the appropriate single-wavenumber representation of the nonlinear energy, the properties which an eligible single-wavenumber representation should have are discussed.

**Key words:** wave turbulence, nonlinear energy, energy budget.

### 1. INTRODUCTION

In the pioneer work by Zakharov [1], it is shown that the dynamics of many wave turbulence systems are governed by Hamiltonians. Complex amplitudes are used as elementary waves in the weak turbulence theory, since they represent linear waves in a canonical representation. The selection of elementary waves determines the form of nonlinear terms in the Hamiltonian, and it reflects the wave interactions of elementary waves. The energy of a wavenumber has been represented as quadratic quantities of the complex amplitudes in studies of the *weak* turbulence systems. Namely, only the linear part of energy has been considered under the assumption of small nonlinearity. However, the integrated quadratic energy, which is obtained by the integration of the quadratic energy over the wavenumbers, is not conserved in general but conserved only in the weakly nonlinear limit.

In the finite nonlinear regime, the quadratic energy is inappropriate for the investigation of the energy budgets because of its nonconservativity. The nonequilibrium statistically-steady state of wave turbulence is realized in the scales called the inertial subrange between energy-input scales and energy-dissipation scales. Then, the energy fluxes estimated by the energy input and/or the energy dissipation [2,3] have sometimes been used to evaluate the energy flux in the inertial subrange. However, such energy fluxes are dominated by the forcing-range statistics and the dissipation-range statistics. The energy flux as well as the energy transfer should be evaluated directly from the nonlinear term of the governing equation. The quadratic-energy flux obtained in first-principle direct numerical simulations, e.g. [4], is non-zero at the smallest or largest wavenumbers.

---

\* Corresponding author, [yokoyama@kuaero.kyoto-u.ac.jp](mailto:yokoyama@kuaero.kyoto-u.ac.jp)

A single-wavenumber representation of the nonlinear energy is indispensable to investigate the energy budget of a wavenumber mode. However, the nonlinear parts of the Hamiltonian consist of the convolution, and they cannot be represented by the nonlinear energy with a single wavenumber in a quadratic form of the complex amplitudes. Recently, a single-wavenumber representation of the nonlinear energy is found in elastic-wave turbulence governed by the Föppl–von Kármán equation [5]. The forward cascade of the energy is reported there in the well-defined manner for the first time, where the detailed energy balance is also confirmed. It is expected to examine how it works in other wave turbulence systems.

To be motivated by the success of the single-wavenumber representation of the nonlinear energy in the elastic-wave turbulence, the properties of such representation are examined here in the Majda–McLaughlin–Tabak (MMT) model [6] as an example of the simplest wave turbulence system. The MMT model is a one-dimensional wave turbulence system that has many interesting characteristics depending on its parameters. It was reported that four statistically-steady states consistent with the weak turbulence theory and one statistically-steady state inconsistent with the theory [6–9]. Moreover, it was also reported that their coexistence and nonlocal interactions in the wavenumber space [7–9], and coherent structures such as solitons, quasisolitons, and quasibreathers [10,11].

Two natural single-wavenumber representations of the nonlinear energy are found in the MMT model, and we will report here numerical results obtained from the two representations. The nonuniqueness of the two single-wavenumber representations of the nonlinear energy in the MMT model results in the different appearances of energy spectra and energy budgets, which stem mainly from the nonlocal interactions among modes. From the viewpoint of the energy budgets, the appropriateness of the single-wavenumber representations is discussed.

## 2. MMT MODEL AND ITS ENERGY

The MMT model is a model for wave turbulence systems which have four-wave nonlinear interactions. In the MMT model, the Hamiltonian is given by the complex amplitudes  $a_k$  as

$$\mathcal{H} = \sum_k |k|^\alpha |a_k|^2 + \frac{\lambda}{2} \sum_{k+k_1-k_2-k_3=0} (|k||k_1||k_2||k_3|)^{-\sigma} a_k^* a_{k_1}^* a_{k_2} a_{k_3}, \quad (1)$$

where the parameter  $\alpha > 0$  determines the linear dispersion relation, and the parameters  $\lambda = \pm 1$  and  $\sigma$  determine the nonlinear interactions. Note that the MMT model can reproduce various kinds of wave turbulence by changing the parameter values. The governing equation of the complex amplitude for a wavenumber  $k \in \mathbb{Z}$  is given as a canonical equation:

$$\frac{\partial a_k}{\partial t} = -i \frac{\delta \mathcal{H}}{\delta a_k^*} = -i |k|^\alpha a_k - i \lambda \sum_{-k_1+k_2+k_3=k} (|k||k_1||k_2||k_3|)^{-\sigma} a_{k_1}^* a_{k_2} a_{k_3}. \quad (2)$$

Note that  $a_k$  is not the complex conjugate of  $a_{-k}$ .

The MMT model has three conservatives: the total energy, the wave action, and the momentum. The total energy is the Hamiltonian of Eq. (1), and the wave action and the momentum are respectively defined as  $\sum_k |a_k|^2$  and  $\sum_k k |a_k|^2$ . It should be emphasized that the total energy, i.e., the Hamiltonian, includes the quartic form of  $a_k$ , while the latter two conservatives are expressed in quadratic forms of the complex amplitudes. We here define the linear energy  $\mathcal{H}^L$  and the nonlinear energy  $\mathcal{H}^N$  respectively for the first and the second terms in the right-hand side of Eq. (1).

If we introduce two auxiliary variables,

$$b_k = \sum_{k_1+k_2=k} (|k_1||k_2|)^{-\sigma} a_{k_1} a_{k_2}, \text{ and } c_k = \sum_{k_1-k_2=k} (|k_1||k_2|)^{-\sigma} a_{k_1}^* a_{k_2}, \quad (3)$$

then the nonlinear part of the Hamiltonian (1) can be rewritten respectively as

$$\mathcal{H}^N = \sum_k \frac{\lambda}{2} |b_k|^2, \quad \text{and} \quad \mathcal{H}^N = \sum_k \frac{\lambda}{2} |c_k|^2. \quad (4)$$

Namely, the nonlinear energy of  $k$  can be defined naturally as a single-wavenumber mode by the two auxiliary variables,

$$E_k^b = \frac{\lambda}{2} |b_k|^2, \quad \text{and} \quad E_k^c = \frac{\lambda}{2} |c_k|^2. \quad (5)$$

As the first step to investigate the energy budget, we focus our attention on the energy transfer and the energy flux. The energy transfer is defined as the time derivative of the energy. Thus, the linear-energy transfer is defined as

$$T_k^L = \frac{\partial E_k^L}{\partial t} = |k|^\alpha a_k^* \frac{\partial a_k}{\partial t} + \text{c.c.} = -i\lambda |k|^\alpha \sum_{-k_1+k_2+k_3=k} (|k||k_1||k_2||k_3|)^{-\sigma} a_k^* a_{k_1}^* a_{k_2} a_{k_3} + \text{c.c.} \quad (6)$$

The total-energy transfers are defined as

$$T_k^{\text{Tb}} = \frac{\partial (E_k^L + E_k^b)}{\partial t} = T_k^L + \left( \frac{\lambda}{2} b_k^* \frac{\partial b_k}{\partial t} + \text{c.c.} \right), \quad \text{and} \quad T_k^{\text{Tc}} = \frac{\partial (E_k^L + E_k^c)}{\partial t} = T_k^L + \left( \frac{\lambda}{2} c_k^* \frac{\partial c_k}{\partial t} + \text{c.c.} \right), \quad (7)$$

where the time derivatives  $\partial b_k / \partial t$  and  $\partial c_k / \partial t$  are obtained by Eqs (2) and (3).

The total-energy fluxes are defined as

$$\mathcal{P}_k^{\text{Tb}} = - \sum_{|k'| \leq k} T_{k'}^{\text{Tb}}, \quad \text{and} \quad \mathcal{P}_k^{\text{Tc}} = - \sum_{|k'| \leq k} T_{k'}^{\text{Tc}}. \quad (8)$$

Because of the energy conservation, the fluxes at the maximal wavenumber are exactly 0, i.e.,  $\mathcal{P}_\infty^{\text{Tb}} = \mathcal{P}_\infty^{\text{Tc}} = 0$ . In other words, these fluxes satisfy  $\mathcal{P}_k^{\text{Tb}} = \sum_{|k'| > k} T_{k'}^{\text{Tb}}$  and  $\mathcal{P}_k^{\text{Tc}} = \sum_{|k'| > k} T_{k'}^{\text{Tc}}$ . After the conventional flux, the linear-energy pseudo-flux can be defined as

$$\mathcal{P}_k^L = - \sum_{|k'| \leq k} T_{k'}^L, \quad (9)$$

though it is not an actual flux but a spurious flux since the linear energy is not conservative. It means that  $\mathcal{P}_\infty^L \neq 0$ . Moreover,  $\mathcal{P}_k^L \neq \sum_{|k'| > k} T_{k'}^L$ .

### 3. NUMERICAL RESULTS

We performed numerical simulations of the MMT model, where external force  $F_k$ , drag  $D_k^s$  and dissipation  $D_k^l$  are added to obtain a statistically-steady state as

$$\frac{\partial a_k}{\partial t} = -i \frac{\delta \mathcal{H}}{\delta a_k^*} + F_k - D_k^s - D_k^l. \quad (10)$$

The periodic boundary condition with  $2\pi$  is assumed. The pseudo-spectral method with the aliasing removal by the 4/2-law is used to obtain the convolution in the nonlinear term. The number of the aliasing-free modes is  $N_{\text{max}} = 2^{14}$ . The random external force  $F_k$  that is time-uncorrelated acts at small wavenumbers  $3 \leq |k| \leq 8$ . The drag  $D_k^s$  is added at smaller wavenumbers as  $D_k^s = \gamma a_k$  for  $|k| \leq 2$ , and the dissipation

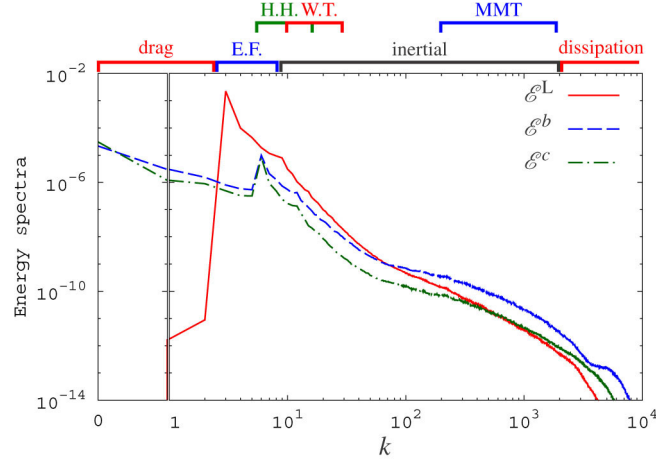


**Fig. 1.** Linear- and nonlinear-energy spectra. The abscissa is linearly scaled for  $k \leq 1$  and logarithmically scaled for  $k \geq 1$ . Each subrange is shown on the top axis: “H.H.,” “W.T.” and “E.F.” stand respectively for the higher harmonics, weak turbulence, and the external force.

$D_k^1$  is added at large wavenumbers as  $D_k^1 = \nu(|k| - k_d)^4 a_k$  for  $|k| > k_d = N_{\max}/8 = 2048$  where  $\gamma$  and  $\nu$  are constant parameters. These ranges do not overlap each other, and the dynamics of the wavenumber modes in the range  $8 < |k| \leq 2048$  is affected by none of external force, drag, and dissipation. The parameters of the MMT model are selected as  $\alpha = 1/2$ ,  $\sigma = -3/4$ , and  $\lambda = 1$  to mimic the deep-water gravity waves [11]. The fourth-order Runge–Kutta method is used for the time integration.

Because of the statistical isotropy, we define the linear-energy spectrum as  $\mathcal{E}_k^L = E_k^L + E_{-k}^L$ , the nonlinear-energy spectrum based on  $b_k$  as  $\mathcal{E}_k^b = E_k^b + E_{-k}^b$ , and that based on  $c_k$  as  $\mathcal{E}_k^c = E_k^c + E_{-k}^c$ . Such spectra obtained in the numerical simulation are drawn in Fig. 1. While the linear energy has large values in the forcing range, the nonlinear energies have in the higher harmonic range  $6 \leq k \leq 16$ . The linear energy is much larger than the nonlinear energies in the energy-containing range. Thus,  $\mathcal{H}^L \gg \mathcal{H}^N$ . On the other hand, the linear energy is much smaller than the nonlinear energies in the drag range. It is due to the fact that the nonlinear energies come from  $a_k$ 's in other ranges. In the dissipation range  $k > k_d = 2048$ , both of the nonlinear energies, based on  $b_k$  and that based on  $c_k$  are larger than the linear energy.

The energy spectra  $\mathcal{E}_k^L$ ,  $\mathcal{E}_k^b$ , and  $\mathcal{E}_k^c$  in the inertial subrange  $10 \lesssim k \lesssim 2 \times 10^3$ , cannot be represented by a single power law. These energy spectra in the smaller wavenumber range  $10 \lesssim k \lesssim 30$  show a very steep power law consistent with the very small nonlinearity there. The modes in this range play the energy source for the modes in the larger wavenumber range  $2 \times 10^2 \lesssim k \lesssim 2 \times 10^3$ , where the linear-energy spectrum  $\mathcal{E}_k^L$  is close to the MMT spectrum, while the nonlinear-energy spectrum  $\mathcal{E}_k^c$  has a less steep slope. Note that the exponent of the MMT spectrum is  $\alpha + 2\sigma - 5/4 = -9/4$  [8].

Though the two nonlinear energies  $\mathcal{E}_k^b$  and  $\mathcal{E}_k^c$  have qualitatively similar forms, they have different values. The nonlinear spectra in the inertial subrange are almost parallel, because the nonlinear energies for a wavenumber  $k$  are written respectively as

$$\begin{aligned} \frac{1}{2} \langle |b_k|^2 \rangle &\approx \sum_{k_1+k_2=k} (|k_1||k_2|)^{-2\sigma} \langle |a_{k_1}|^2 \rangle \langle |a_{k_2}|^2 \rangle, \\ \frac{1}{2} \langle |c_k|^2 \rangle &\approx \frac{1}{2} \sum_{k_1+k_2=k} (|k_1||k_2|)^{-2\sigma} \langle |a_{k_1}|^2 \rangle \langle |a_{k_2}|^2 \rangle + \frac{1}{2} \delta_{k,0} \left( \sum_{k_1} |k_1|^{-2\sigma} \langle |a_{k_1}|^2 \rangle \right), \end{aligned} \tag{11}$$

if the random phase approximation can be applied over all the wavenumbers and the system is statistically isotropic. In fact, as shown in Fig. 1,  $\mathcal{E}_k^c \approx \mathcal{E}_k^b/2$  in the range  $10 < k < 30$ , where the nonlinearity is weak, while  $\mathcal{E}_k^c \ll \mathcal{E}_k^b$  in the range  $k > 10^2$ , where the nonlinearity is relatively strong. This result suggests the

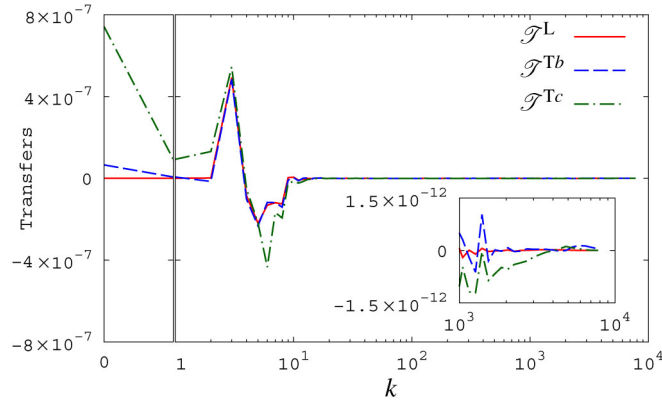


**Fig. 2.** Linear-energy transfer and total-energy transfers. The inset shows the enlargement of the dissipation range. The abscissa is linearly scaled for  $k \leq 1$  and logarithmically scaled for  $k \geq 1$ .

existence of nonlocal direct interactions from  $c_0$  in the representation of the auxiliary variable  $c_k$ . The largest values of the nonlinear energies appear at  $k = 0$ . The nonlinear energies of the zero mode are written as  $E_0^b = |b_0|^2/2 = |\sum_{k'} |k'|^{-2\sigma} a_{k'} a_{-k'}|^2/2$  and  $E_0^c = |c_0|^2/2 = |\sum_{k'} |k'|^{-2\sigma} |a_{k'}|^2|^2/2$ . Thus,  $0 \leq E_0^b \leq E_0^c$ , which is proven by the Cauchy–Schwarz inequality. Our numerical simulation shows  $E_0^b \approx 2.2 \times 10^{-5}$  and  $E_0^c \approx 3.1 \times 10^{-5}$ . Since both summations in Eq. (4) give the same nonlinear part of the Hamiltonian, the relation  $\mathcal{E}_k^b > \mathcal{E}_k^c$  holds for most wavenumbers. In fact,  $\mathcal{E}_k^b$  is much larger than  $\mathcal{E}_k^c$  mostly, and it is inconsistent with Eq. (11), i.e., the weak turbulence theory.

As is the case with the energy spectra, we define three energy transfers: the linear-energy transfer,  $\mathcal{T}_k^L = T_k^L + T_{-k}^L$ , the total-energy transfer based on  $b_k$ ,  $\mathcal{T}_k^{Tb} = T_k^{Tb} + T_{-k}^{Tb}$ , and the total-energy transfer based on  $c_k$ ,  $\mathcal{T}_k^{Tc} = T_k^{Tc} + T_{-k}^{Tc}$ . These transfers are drawn in Fig. 2. The energy transfers have large magnitudes in the forcing range  $3 \leq k \leq 8$ , though the fluctuations are very large. The positive and negative values seen there show that the energy budget is not so simple even in the forcing range. The modes in the positive range receive energy while the modes in the negative range provide energy, though the all-inclusive representations (6) and (7) cannot resolve whether it is due to the random external forces or to the nonlinear interactions. Although the values in the dissipation range  $k \gtrsim 2 \times 10^3$  are difficult to see in Fig. 2, the amounts of them are statistically the same as that of energy input because of the steadiness of the system, which can be recognized by considering the wide horizontal range. The transfers,  $\mathcal{T}_k^{Tb}$  and  $\mathcal{T}_k^L$ , are positive in the dissipation range, and the former is much larger than the latter. The transfer  $\mathcal{T}_k^{Tc}$ , however, changes its sign from negative to positive in the dissipation range.

The transfer  $\mathcal{T}_k^{Tc}$  is much different from the other two  $\mathcal{T}_k^{Tb}$  and  $\mathcal{T}_k^L$ . At  $k = 0$ , both  $\mathcal{T}_0^{Tb}$  and  $\mathcal{T}_0^{Tc}$  are positive, because the zero modes of the nonlinear energies receive energy while that of the linear energy cannot by definition. For  $\mathcal{T}_k^{Tc}$ , furthermore, the large positive values appear in the drag range and the negatively large values appear in the forcing range. In the inertial subrange, the values of  $\mathcal{T}_k^{Tc}$  is always negative, while the values of  $\mathcal{T}_k^{Tb}$  fluctuate around 0. In this sense, there exists no range where the energy cascades if we use  $c_k$  as the auxiliary variable.

The linear-energy pseudo-flux and the total-energy fluxes are drawn in Fig. 3. The linear-energy pseudo-flux is spurious because it breaks the energy conservation [4]. Therefore, the pseudo-flux is physically inappropriate, because it stems from the continuity equation of energy. Both of the total-energy fluxes are 0 at the maximal wavenumber, and are consistent with the energy conservation. However, their values at other wavenumbers are completely different. In the inertial range, the values of  $\mathcal{P}_k^{Tb}$  are positive and almost constant, while those of  $\mathcal{P}_k^{Tc}$  are negative and increase as the wavenumbers become large. These negative values of  $\mathcal{P}_k^{Tc}$  result from the negatively large value of the flux at  $k = 0$ . It reflects the large value of the energy transfer there shown in Fig. 2.

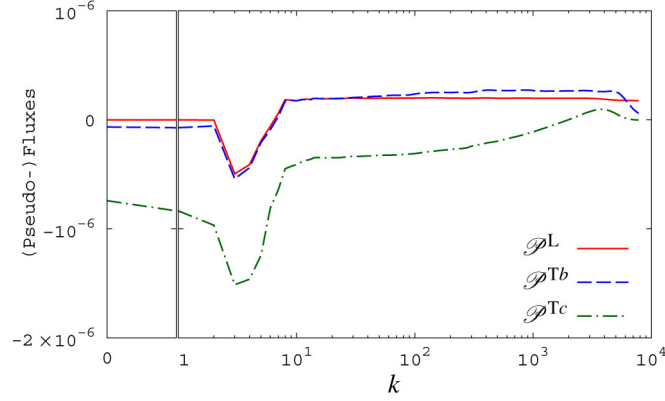


**Fig. 3.** Linear-energy pseudo-flux and total-energy fluxes. The abscissa is linearly scaled for  $k \leq 1$  and logarithmically scaled for  $k \geq 1$ .

Figure 3 indicates that the total-energy fluxes depend on which mode is selected as an elementary wave. When one uses  $b_k$  as an elementary wave, we observe that the wave field receives the energy from the external force, the energy cascades in the inertial subrange, and the energy is dissipated in the dissipation range. When one uses  $c_k$  as an elementary wave, on the other hand, the large contribution of the total-energy transfer at  $k = 0$  and the non-constancy of the total-energy flux in the inertial subrange suggest that the energy is not transferred as step-by-step cascades, but by nonlocal interactions in the wavenumber space. These difference appears also in Fig.1: the power spectrum of  $\mathcal{E}_k^c$  around  $k \approx 10^3$  is shallower and wider than that of  $\mathcal{E}_k^b$ . In the range  $20 \lesssim k \lesssim 200$ , both total-energy fluxes  $\mathcal{P}_k^{Tb}$  and  $\mathcal{P}_k^{Tc}$ , similarly to the nonlinear-energy spectra  $\mathcal{E}_k^b$  and  $\mathcal{E}_k^c$ , are almost parallel, but their values and even their signs are different, as seen in Fig. 3.

#### 4. CONCLUDING REMARKS

The single-wavenumber representations of the nonlinear energy in the wave turbulence systems is examined in the MMT model in order to take our understanding in [5] one step further. The two natural single-wavenumber representations of the nonlinear energy are found in the MMT model. One is based on an auxiliary variable  $b_k = \sum_{k_1+k_2=k} (|k_1||k_2|)^{-\sigma} a_{k_1} a_{k_2}$ , and the other on the other auxiliary variable  $c_k = \sum_{k_1-k_2=k} (|k_1||k_2|)^{-\sigma} a_{k_1}^* a_{k_2}$ . The two natural representations indicate that the representations are not necessarily unique in the MMT model. It is in contrast with the unique representation in the elastic-wave turbulence, reported in [5].

Our numerical simulation of the MMT model reveals the following facts. While the two kinds of the nonlinear-energy spectra are qualitatively similar, the two total-energy transfers as well as the two total-energy fluxes are different at the zero mode and in the inertial subrange. The most noticeable difference is that the total-energy flux based on  $c_k$  is not constant in the inertial subrange while that based on  $b_k$  is constant. Furthermore, even their signs are different from each other.

The differences come mainly from the interactions between the zero mode and other modes. The zero mode of  $b_k$ , i.e.,  $b_0 = \sum_k |k|^{-2\sigma} a_k a_{-k}$  comes from the interaction between  $a_k$  and  $a_{-k}$ . On the other hand, the zero mode of  $c_k$ , i.e.,  $c_0 = \sum_k |k|^{-2\sigma} |a_k|^2$  comes from the selfinteraction of  $a_k$ . The apparent nonlocal interactions between  $c_0$  and  $a_k$  (and  $c_k$ ) where the wavenumber  $k$  is in the inertial subrange make the nonconstant energy flux of  $\mathcal{P}^{Tc}$  in the inertial subrange. If we believe the energy cascade, the auxiliary variable  $b_k$  is preferable to  $c_k$ . However, the nonlocal interactions are reported in the focusing MMT model with  $\lambda = -1$  [8], and the nonlocal interactions might play a dominant role in the present system. Therefore, the appropriateness of the representation including the possibility of a more appropriate auxiliary variable should be judged carefully.

Lastly, it may be interesting to point out that if  $a_k$  were complex conjugates of  $a_{-k}$  such as the Fourier coefficient of a real variable, the auxiliary variables  $b_k$  and  $c_k$  would become complex conjugates of each other as known from the definition (3). In this sense, the differences observed above stem from the non-conjugacy of  $a_k$  with  $a_{-k}$ . The MMT model as well as the auxiliary variables  $b_k$  and  $c_k$  is merely mathematical and arbitrary to some extent. The nonlinear energy in the MMT model is in contrast to that in the elastic-wave turbulence [5], which gives the stretching energy and has a physical meaning itself. If we restrict the initial conditions of  $a_k$  and the external force  $F_k$  to have this complex conjugacy in the MMT model, the nonlinear energies based on the two auxiliary variables become identical, and we may be able to investigate the energy budget in more detail. Furthermore, we can develop the MMT model by considering the physically plausible characteristics. The study along this line is currently in progress and will be reported elsewhere.

## ACKNOWLEDGEMENTS

Numerical computation in this work was carried out at the Yukawa Institute Computer Facility. This work was partially supported by JSPS KAKENHI grant No. 25400412.

## REFERENCES

1. Zakharov, V. E., L'vov, V. S., and Falkovich, G. *Kolmogorov Spectra of Turbulence I: Wave Turbulence*. Springer-Verlag, Berlin, 1992.
2. Dias, F., Guyenne, P., and Zakharov, V. E. Kolmogorov spectra of weak turbulence in media with two types of interacting waves. *Phys. Lett. A*, 2001, **291**, 139–145.
3. Miquel, B., Alexakis, A., and Mordant, N. Role of dissipation in flexural wave turbulence: from experimental spectrum to Kolmogorov–Zakharov spectrum. *Phys. Rev. E*, 2014, **89**, 062925.
4. Rumpf, B. and Biven, L. Weak turbulence and collapses in the Majda–McLaughlin–Tabak equation: fluxes in wavenumber and in amplitude space. *Physica D*, 2005, **204**, 188–203.
5. Yokoyama, N. and Takaoka, M. Single-wave-number representation of nonlinear energy spectrum in elastic-wave turbulence of the Föppl–von Kármán equation: energy decomposition analysis and energy budget. *Phys. Rev. E*, 2014, **90**, 063004.
6. Majda, A. J., McLaughlin, D. W., and Tabak, E. G. A one dimensional model for dispersive wave turbulence. *J. Nonlinear Sci.*, 1997, **7**, 9–44.
7. Cai, D. and McLaughlin, D. W. Chaotic and turbulent behavior of unstable one-dimensional nonlinear dispersive waves. *J. Math. Phys.*, 2000, **41**, 4125–4153.
8. Cai, D., Majda, A. J., McLaughlin, D. W., and Tabak, E. G. Spectral bifurcations in dispersive wave turbulence. *Proc. Natl. Acad. Sci. USA*, 1999, **96**, 14216–14221.
9. Cai, D., Majda, A. J., McLaughlin, D. W., and Tabak, E. G. Dispersive wave turbulence in one dimension. *Physica D*, 2001, **152–153**, 551–572.
10. Zakharov, V. E., Guyenne, P., Pushkarev, A. N., and Dias, F. Wave turbulence in one-dimensional models. *Physica D*, 2001, **152–153**, 573–619.
11. Pushkarev, A. and Zakharov, V. E. Quasibreathers in the MMT model. *Physica D*, 2013, **248**, 55–61.

## Mittelineaarsete lainete energia turbulentsi tüüpi lainesüsteemides

Naoto Yokoyama ja Masanori Takaoka

Turbulentsi tüüpi mittelineaarsete lainesüsteemide üksikute komponentide energia bilansi ja mittelineaarsete interaktsioonide põhjustatud energiavahetuse arutamisel on tarvis klassikaline (lainekõrguse ruuduga võrdeline) energia kontseptsioon asendada keerukama mittelineaarse funktsiooniga. On näidatud, et selline üldistus pole ühene ja võivad eksisteerida erinevad, kuigi teatavas mõttes ekvivalentsed võimalused. Näitena on vaadeldud Majda–McLaughlini–Tabaki mudelit. Üksikute laine komponentide kompleksseid amplituude

esitavaid abimuutujaid saab selle mudeli raames konstrueerida mitmel moel. Komponentide energia kirjeldamiseks on vaadeldud kaht mõistlikku alternatiivi. Arvutisimulatsioonide abil on näidatud, et energia selliste mittelineaarsete analoogide spektrid on kvalitatiivselt sarnased, kuid nii üksikute lainekomponentide energia kui ka interaktsioonides edasi kanduv energia võib erinev olla. On visandatud selliste piirangute võimalused, mille korral üksikute lainekomponentide energia üldistust saaks üheselt määratleda.